JOURNAL OF MATERIALS SCIENCE **36** (2001) 3179–3188

Fabrication and characteristics of AA6061/SiC_p composites by pressureless infiltration technique

K. B. LEE, H. S. SIM
School of Metallurgical and Materials Engineering, Kookmin University, Seoul 136-702, Korea
E-mail: kblee@kmu.kookmin.ac.kr

S. H. KIM, K. H. HAN
School of Metallurgical and Materials Engineering, Youngnam University, Kyungsan, Kyungsangbuk-do 712-749, Korea

H. KWON
School of Metallurgical and Materials Engineering, Kookmin University, Seoul 136-702; Center for Advanced Aerospace Materials, POSTECH, Pohang 790-784, Korea

The tensile properties and microstructures of AA6061/SiC_p composites fabricated by the pressureless infiltration method under a nitrogen atmosphere were examined. Since the spontaneous infiltration of molten AA6061 into the powder bed containing SiC_p occurred at 800 °C for 1 hour under a nitrogen atmosphere, it was possible to fabricate composites reinforced with SiC_p. Reaction product (Al_4C_3) was formed at the interface between SiC_p and Al alloy matrix. In addition, the amount and size of the Al_4C_3 is increased significantly by increasing the infiltration temperature. The reaction product (AlN) was formed as a result of the *in situ* reaction in both the control alloy and the composite. A significant strengthening even in the control alloy occurred due to the formation of *in situ* AlN particle even without an addition of SiC_p. While a further strengthening of the composite was produced by the reinforced SiC_p, strain to failure of the composite fabricated at 800 °C showed the lowest value (1.3%) in the T6 condition due to the formation of the severe reaction product (Al_4C_3). The grain size of the control alloy significantly decreased to about 20 μm compared to 50 μm for the commercial alloy. In addition, the grain size in the composite reinforced with SiC_p further decreased to about 8.0 μm. This grain refinement contributed to strengthening of the control alloy and composite.

1. Introduction

Metal matrix composites (MMCs) reinforced with ceramic phase have become of great interest because of the combined effects of metallic and ceramic materials relative to the corresponding monolithic alloys. Thus various fabrication methods have been developed, such as powder metallurgy, stir casting, pressure infiltration method, etc. Furthermore, in recent years there has been a growing interest in the development of technologies for the *in situ* production of MMCs, such as Lanxide's PRIMEX™ process, Martin Marietta's XD™ process, self-propagating high-temperature synthesis (SHS) and reactive-gas injection [1–15].

Al composites reinforced with SiC particles are very attractive for their properties, such as high modulus, high specific stiffness, high-temperature resistance, low coefficient of thermal expansion, good wear resistance, and good workability. In the last decade, therefore, significant studies were conducted on their mechanical properties and interfacial reaction in SiC/Al composites fabricated by various processing methods, containing compocasting, squeeze casting, powder metallurgical hot pressing, and spray forming. etc [16–21]. However, few publications on the pressureless infiltration process (PRIMEX process) have appeared because of the existence of patents for this proprietary process, even though it has many advantages relative to conventional MMC fabrication techniques.

The PRIMEX process is an innovative technique for fabricating MMCs by the spontaneous infiltration of molten Al alloy containing Mg into a ceramic filler or preform under a nitrogen atmosphere without the aid of vacuum or externally applied pressure [5–15]. For the pressureless infiltration in this process, both nitrogen and Mg should be needed. Previous studies have investigated that the spontaneous infiltration of molten Al alloy to provide the matrix of Al composites in this process is influenced by Mg content, additional alloying elements, nitrogen concentration in the gas atmosphere, infiltration temperature and time, etc. [5–10]. In particular, at least 1 wt pct, and preferably 3 wt pct, Mg is required.

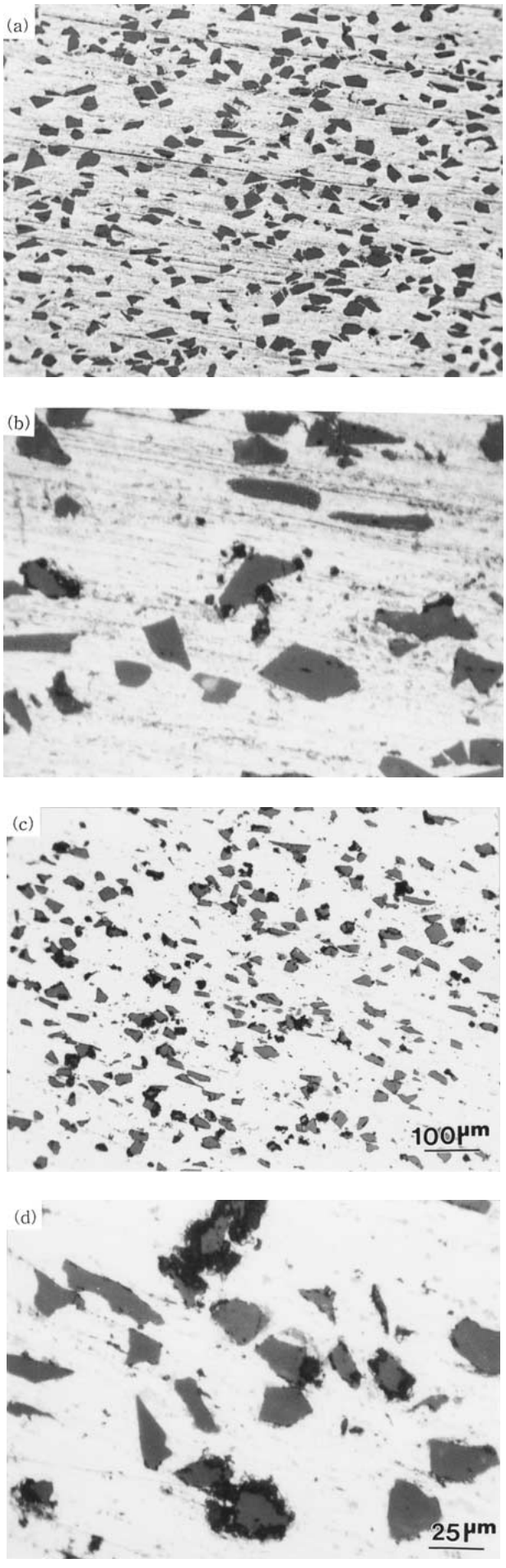

Figure 1 Optical micrographs showing the distribution of reinforcement and reaction product in AA6061/SiC_p composites fabricated at 700 °C ((a), (b)) and 800 °C ((c), (d)), respectively.

Because the interface reaction and mechanical properties in Al/SiC depends on several fabrication parameters (for example, temperature, holding time, atmosphere and chemical composition of both the Al matrix and the SiC reinforcement), the characteristics of composites fabricated will be changed, depending on the fabrication procedure and composite system [18]. Therefore, in this study, AA6061/SiC_p composites were fabricated by the pressureless infiltration method, and the tensile properties and interfacial reaction were investigated.

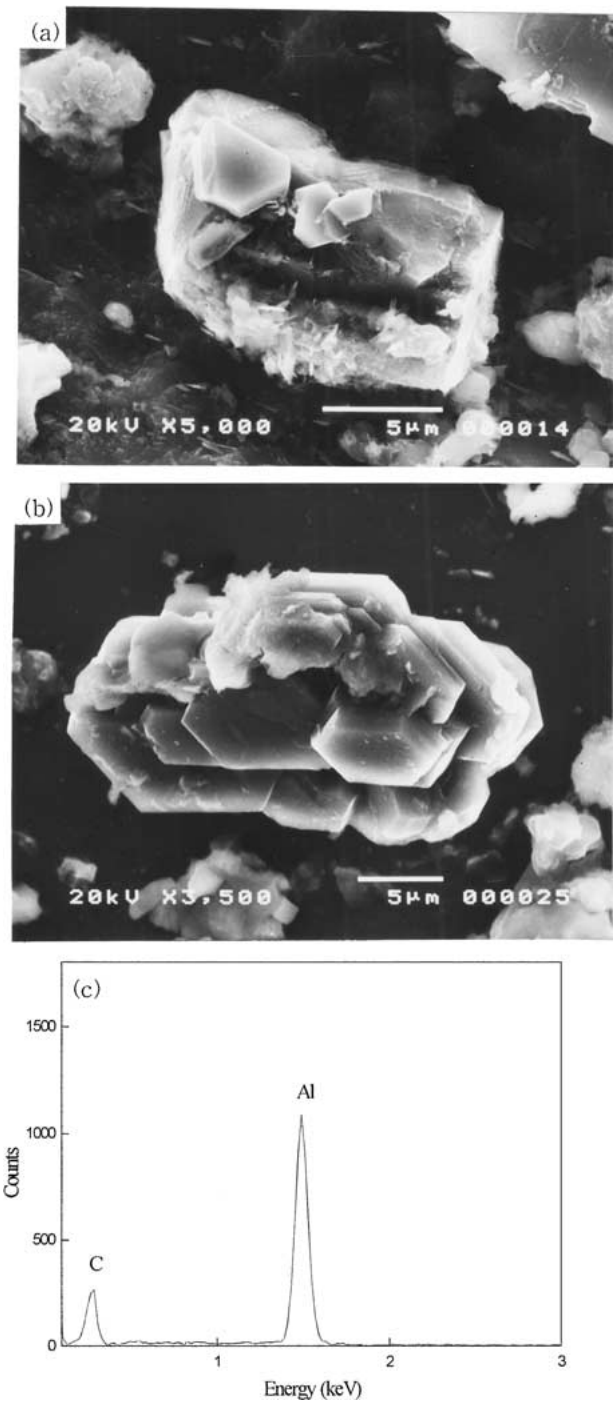

Figure 2 SEM micrographs and EDS profile showing the Al_4C_3 reaction products, after dissolving away the Al alloy matrix in the composites fabricated at: (a) 700 °C and (b) 800 °C.

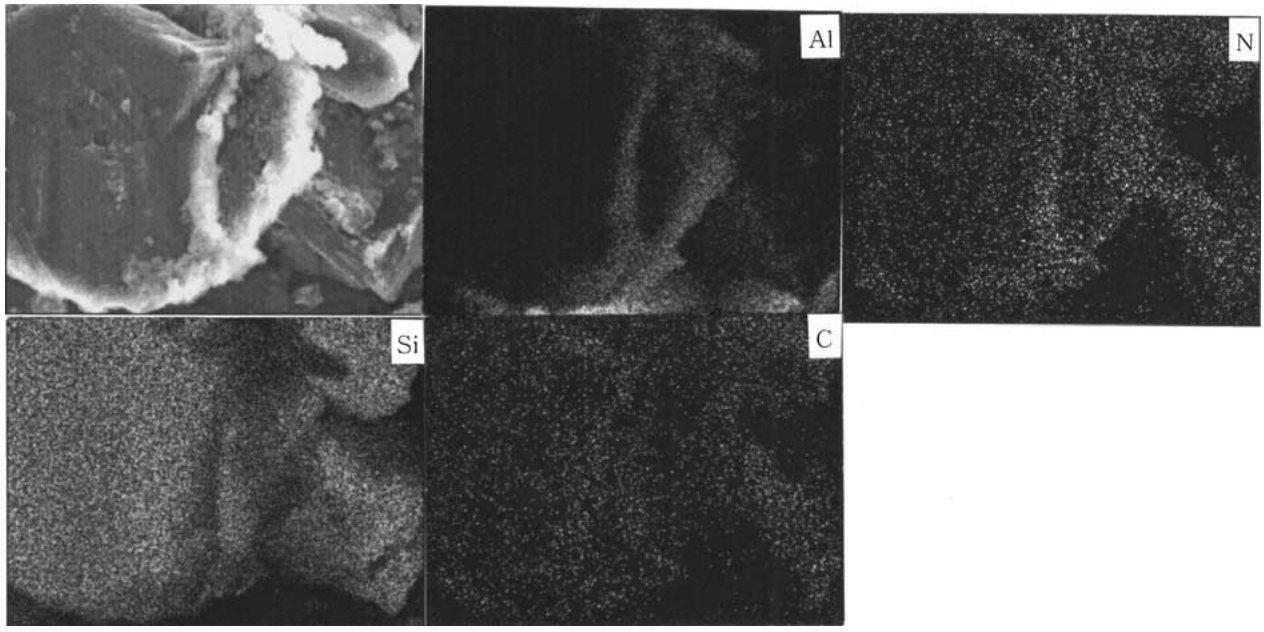

Figure 3 Secondary electron image and elemental dot-mapping images observed by EDS in the composite.

2. Experimental procedure

The average size of Al, Mg and SiC particles used in this study was about 50, 13, and 22 μm, respectively. After these powders (Al-1.2wt.%Mg-0.8wt%Si-20vol.%SiC) were blended by roll mixing in an alumina jar, the powder mixture was put into a crucible. A 6061 Al ingot was placed on this powder bed. This assembly was heated to 700 and 800 °C, and held for 1 hour under a flowing nitrogen atmosphere in the retort furnace (5000 cc/min). Then the assembly was cooled to about 600 °C under the nitrogen atmosphere, in order to inhibit oxidation during solidification, and was removed from the furnace. The schematic arrangement employed for the composite fabrication in this study is given elsewhere [11–15].

For comparison, the control AA6061 was made through the same route, using a powder bed without the SiC_p. Both of these ingots were extruded at 450 °C into a bar 16 mm in diameter (extrusion ratio 22 : 1). Tensile specimens having a gauge length of 25 mm and 2 mm thickness were machined from the extruded bars, parallel to the extrusion direction. Those specimens were heat treated to the T6 condition (529 °C-2 h solution treatment, water quenching and 177 °C, 6–8 h aging). Tensile testing was performed at room temperature, using a cross-head speed of 1mm/min. Average tensile data were obtained from at least five tests for each condition.

The resulting microstructures and reaction products were investigated using scanning electron microscopy (SEM), and transmission electron microscopy (TEM). For the SEM analysis of the reaction products, specimens were prepared by dissolving away the metal matrix in a solution of methanol bromine and examined using a JEOL 1210LV SEM equipped with an energy dispersive X-ray spectrometer (EDS) operated at 20 kV. Thin foils for TEM analysis were ground mechanically to a thickness of about 60 μm and then punched to into 3 mm diameter discs. Finally, the discs were thinned using dimpling and ion milling (5 kV, at a tilt angle of 4–6°). All samples were examined by JEOL 1210 TEM coupled to an EDS system operated at 120 kV.

3. Results and discussion

3.1. Microstructural analysis

The spontaneous infiltration of molten metal at 800 °C for 1 hour under a nitrogen atmosphere made it possible to fabricate 6061 Al matrix composite reinforced with SiC_p as well as control 6061 Al without SiC_p. The spontaneous infiltration behavior was explained in detail in previous papers [11–15].

Fig. 1a and c show the relatively uniform distribution of the SiC particles in the Al alloy matrix of composites fabricated at 700 and 800 °C, respectively. The volume fraction of SiC particles was about 15 and 16%, measured by point-count method. In the magnified image of Fig. 1a and b, it can be seen that reaction products were formed at interface between SiC_p and Al alloy matrix. In addition, interfacial reaction increased by increasing the infiltration temperature and thus SiC particles were more severely attacked by the Al melt during fabrication of MMC (Fig. 1d).

Fig. 2 shows the reaction products observed by SEM in composites fabricated at 700 and 800 °C, respectively, after Al alloy matrix was dissolved away with a solution of methanol bromine. Similar to Fig. 1, a great amount of reaction product was clearly observed on the surface of the SiC particle in the composite fabricated at 800 °C (Fig. 2b). From the EDS analysis, these reaction products were identified as Al_4C_3, and Al_4C_3 coarsely grew to the typical hexagonal morphology.

The reaction between molten Al and SiC_p has been investigated by many authors [16–21]. The Al/SiC

interface exhibits a good chemical stability at temperature lower than about 870 K, whereas it becomes reactive at temperature where Al is in the liquid state, i.e. at temperature higher than 833 K. SiC reacts with molten Al according to the reactions, $4Al + 3SiC = Al_4C_3 + 3Si$ [19].

Because the solubility of [C] in liquid Al is very low at temperature from 660 to 800 °C, the threshod carbon activity values for Al_4C_3 formation are small. The carbon atoms that go into solution will react almost immediately with Al to form, Al_4C_3 [21]. Although bonding between SiC and Al_4C_3 appears to be good, the Al_4C_3-SiC interface is generally rough and can lead to regions of stress localization. Interfacial reaction in SiC_p/Al composites is known to have several undesirable effects on the overall composite properties: (i) composites can be susceptible to corrosive environments owing to the presence of Al_4C_3, because Al_4C_3 is unstable in some environments such as water, methanol, and HCl, etc.; (ii) degradation of SiC itself occurs owing to the formation of Al_4C_3; and (iii) the elemental Si, formed as a result of the interfacial reaction, produces the Al-Si eutectic during fabrication or the heat treating stage, resulting in undesired mechanical and physical properties of the matrix alloy. Therefore it may be desirable to prevent the formation of Al_4C_3. Generally, two methods have been accepted widely: addition of Si into the Al matrix and the pre-treatment of SiC to produce a SiO_2 layer on the surface of the SiC [16].

Fig. 3 shows secondary electron image and elemental dot-mapping images of composite. It can be seen that N is enriched but Al is deficient on the surface of the SiC particle. Formation of the AlN is related to fabrication method of MMC (e.g. pressureless infiltration technique) used in this study. It is suggested that Mg vapor (serving as an infiltration enhancer precursor) react with nitrogen to form Mg_3N_2 coating (which serves as infiltration enhancer) around the particles in the preform or filler [10]. This Mg_3N_2 may lead to a spontaneous infiltration of molten Al alloy *via* great enhancement of wetting between molten alloy and reinforcement. In addition, this Mg_3N_2 reacts with molten Al and thus AlN is formed as a result of the *in situ* reaction ($Mg_3N_2 + 2Al = 2AlN + 3Mg$). Lee and Kwon indirectly demonstrated that the formation of Mg_3N_2 is necessary to induce spontaneous infiltration [11–15]. The AlN was also observed in previous studies of all composite systems, such as Al/Al_2O_3, Al/BN, Al/Si_3N_4, Al/B_4C etc, fabricated by the same pressureless infiltration method [11–15].

Fig. 4 shows secondary electron images and EDS profile of the reaction product obtained in the control alloy after dissolving away the Al alloy matrix with a solution of methanol bromine. A great amount of reaction product (whose size was about 1.0 μm) was clearly observed on the surface of the old Al particles that had composed the powder bed prior to infiltration. After extrusion, this was, of course, aligned along the extrusion direction as shown in Fig. 4b. The EDS analysis revealed only Al and N, and the atomic ratio of Al to N was around one, coincident with the stoichiometry of AlN. Fig. 5 shows bright field and dark field images, and selected area diffraction patterns (SADP) of the reaction product observed by TEM in both control alloy and composite. This reaction product was identified as AlN with a hexagonal structure and lattice parameters, $a = 3.086$ nm and $c = 4.938$ nm in the control alloy and $a = 3.093$ nm and $c = 4.949$ nm in the composite (theoretical value $a = 3.1114$ nm and $c = 4.9792$ nm, space group: $P6_3mc$) [22].

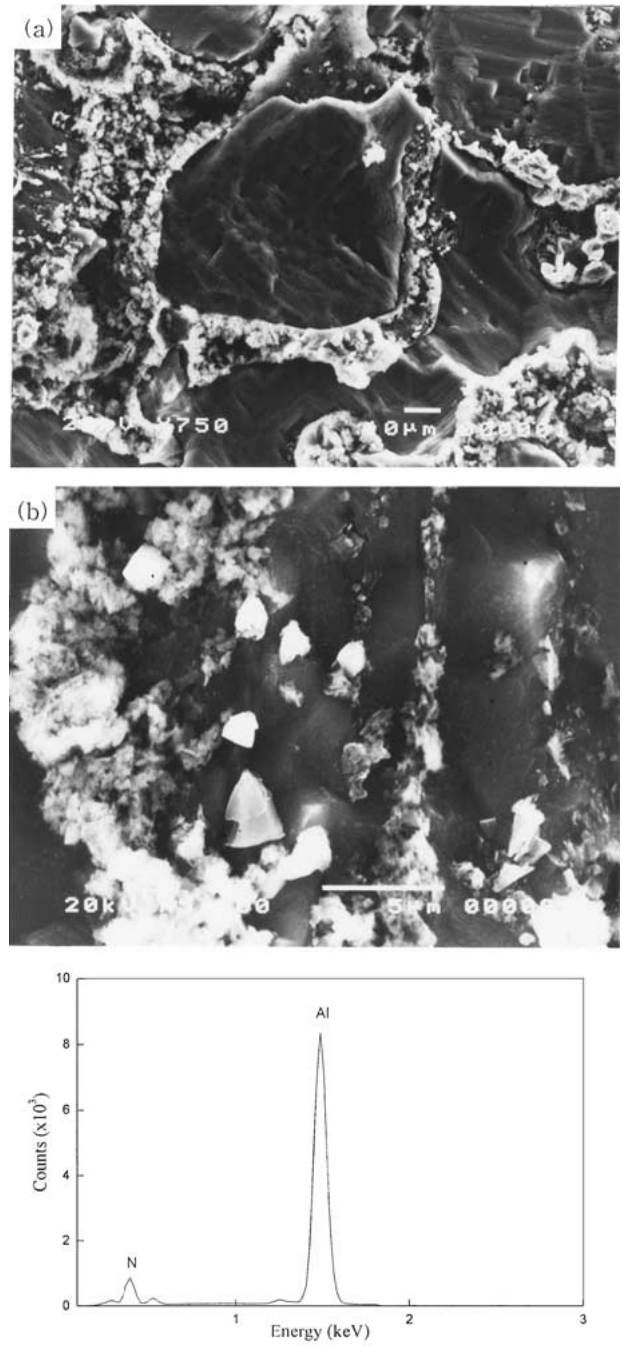

Figure 4 SEM micrographs and EDS profile showing the AlN reaction products, after dissolving away the Al alloy matrix in the control alloy: (a) as-fabricated and (b) extruded condition.

Fig. 6 shows SEM micrographs and EDS profile of another reaction product observed in both the control alloy and composite. According to the analytical results obtained from EDS analysis, the particle of polyhedron morphology was identified as $MgAl_2O_4$. Oxide films on Al and SiC particles in the powder mixture can provide a source of oxygen for formation of $MgAl_2O_4$. Phase

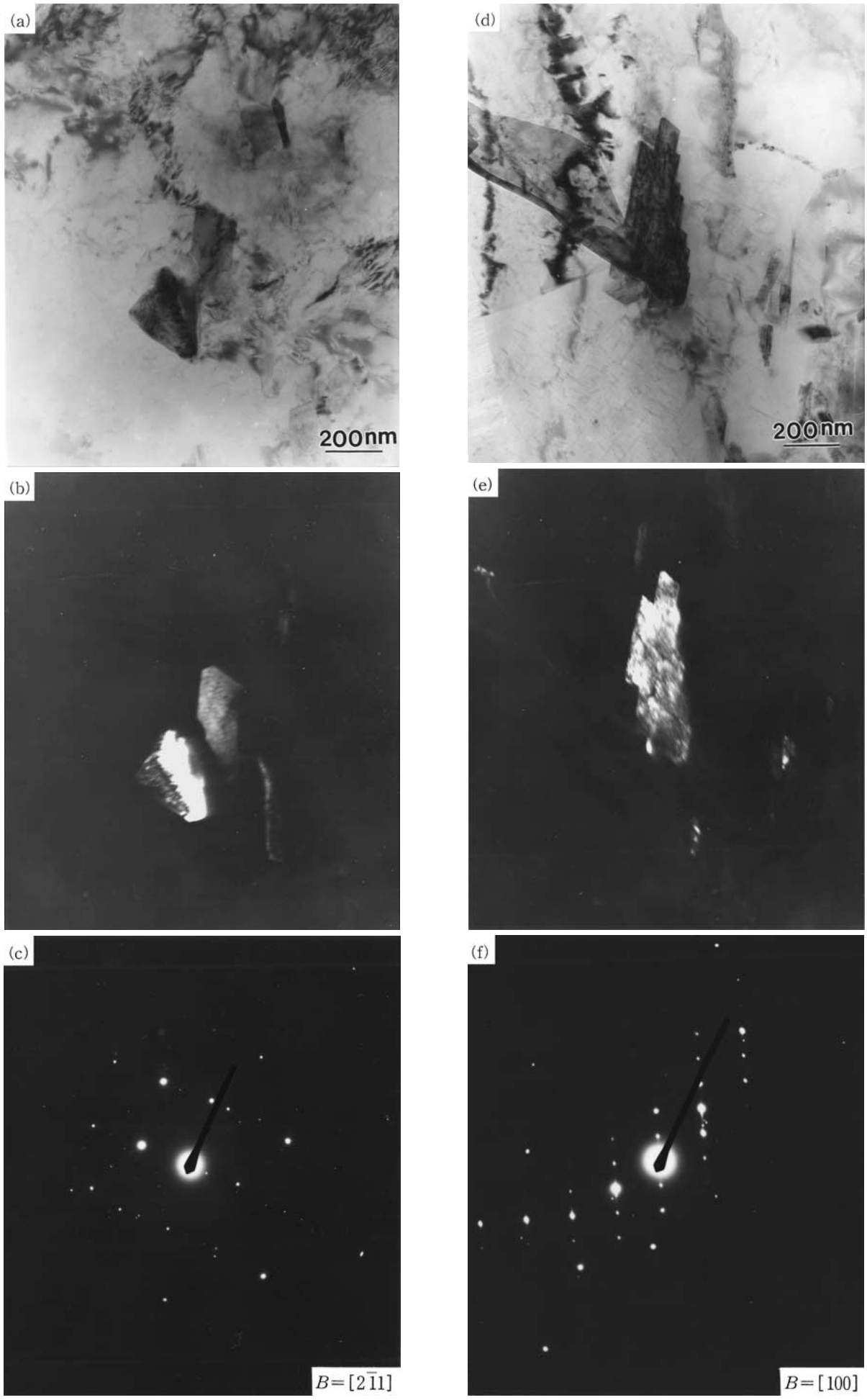

Figure 5 TEM micrographs showing reaction products, AlN: (a) BF, (b) DF, and (c) SADP in control alloy, and (d) BF, (e) DF, and (f) in the composite, respectively.

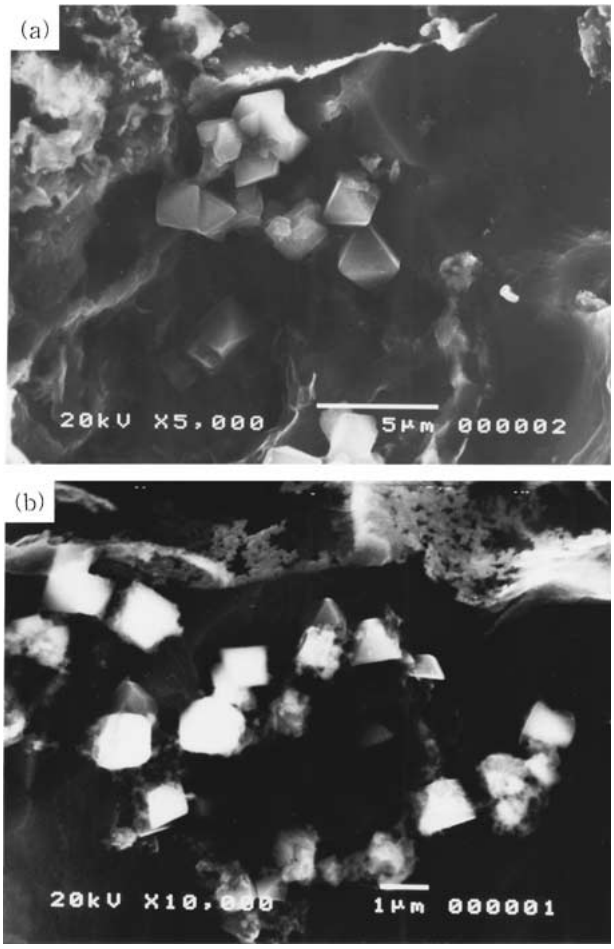

Figure 6 SEM micrographs and EDS profile showing $MgAl_2O_4$ after dissolving away the Al alloy matrix: (a) control alloy and (b) composite.

identified from EDS analysis was also confirmed using TEM. Fig. 7 shows the bright, dark field images, and selected area diffraction patterns of the reaction product observed in the control alloy and composite, respectively. The reaction product was identified as the $MgAl_2O_4$ of cubic structure with the measured lattice parameter, $a = 7.848$ and 8.128 nm (theoretical value, 8.0831 nm, space group: $Fd3m$) [22].

3.2. Tensile properties

Several theories and mechanisms have been suggested to explain the strengthening of MMCs. However, generally the strength of the composites does not depend on a unique mechanism but several mechanisms may be act simultaneously [23]. At present study, strengthening effect both the control alloy and the composites is analyzed in terms of the refinement of the matrix grain size and reinforcement effect (artificially added SiC and *in situ* formed AlN).

Fig. 8 and Table I show the variation of tensile strength with aging time at 177 °C in commercial AA6061, control AA6061 and composites which were solution treated for 2 hours at 529 °C. The tensile strength in the control AA6061 was 55–70 MPa greater than the commercial AA6061. These values were an additional 84–99 MPa higher in the composite reinforced with SiC compared to the control alloy. A large increase in strength in the case of the control AA6061 is related to the *in situ* formation of AlN particles. As previously mentioned, when the MMCs were fabricated by pressureless infiltration technique, AlN is formed as a result of the *in situ* reaction ($Mg_3N_2 + 2Al = 2AlN + 3Mg$). Furthermore, these AlN particles intimately contact with the matrix and also show clean interface (Fig. 5), as well the size of AlN is very fine. This means that AlN particles *in situ* formed are thermodynamically stable in the matrix, as well no wettability problem.

The grain size was measured by linear intercept method in order to investigate its effect on the strength of the materials. The grain size of the control alloy is decreased significantly to about 20 μm compared to 50 μm for the commercial alloy. In addition, the grain size in the composite reinforced with SiC is further decreased to about 8.0 μm. This grain refinements contributed to strengthening of the control alloy and composite as well. Fig. 9 shows the subgrain structures observed by TEM in the solution treated condition. The sungrain size of the composite was smalller than that of the commercial alloy. It is well known that in particle-reinforced MMCs, the grain size is generally small compared to an unreinforced material of similar composition, and it has been shown that particle-stimulated nucleation (PSN), coupled with particle pinning during normal grain growth, is responsible for this small grain size [24, 25].

However, strain to failure of the composite significantly is decreased compared to that for the alloy. Interfacial reaction increased by increasing the infiltration temperature and thus the amount and size of the reaction products (Al_4C_3) formed in the composite fabricated at 800 °C greatly increased when compared to

TABLE I Tensile properties of commercial, control alloy, and composites

	UTS (MPa)		YS (MPa)		El (Pct)	
Material Designations	ST	T6	ST	T6	ST	T6
Commercial AA6061	220	312	104	271	15.1	6.8
Control AA6061	290	367	209	323	10.8	6.2
AA6061/SiC composite (700 °C)	292	451	183	419	7.2	3.1
AA6061/SiC composite (800 °C)	290	458	194	422	6.5	1.3

ST: solution-treated condition UTS: ultimate tensile strength,
YS: 0.2% offset yield strength El: elongation

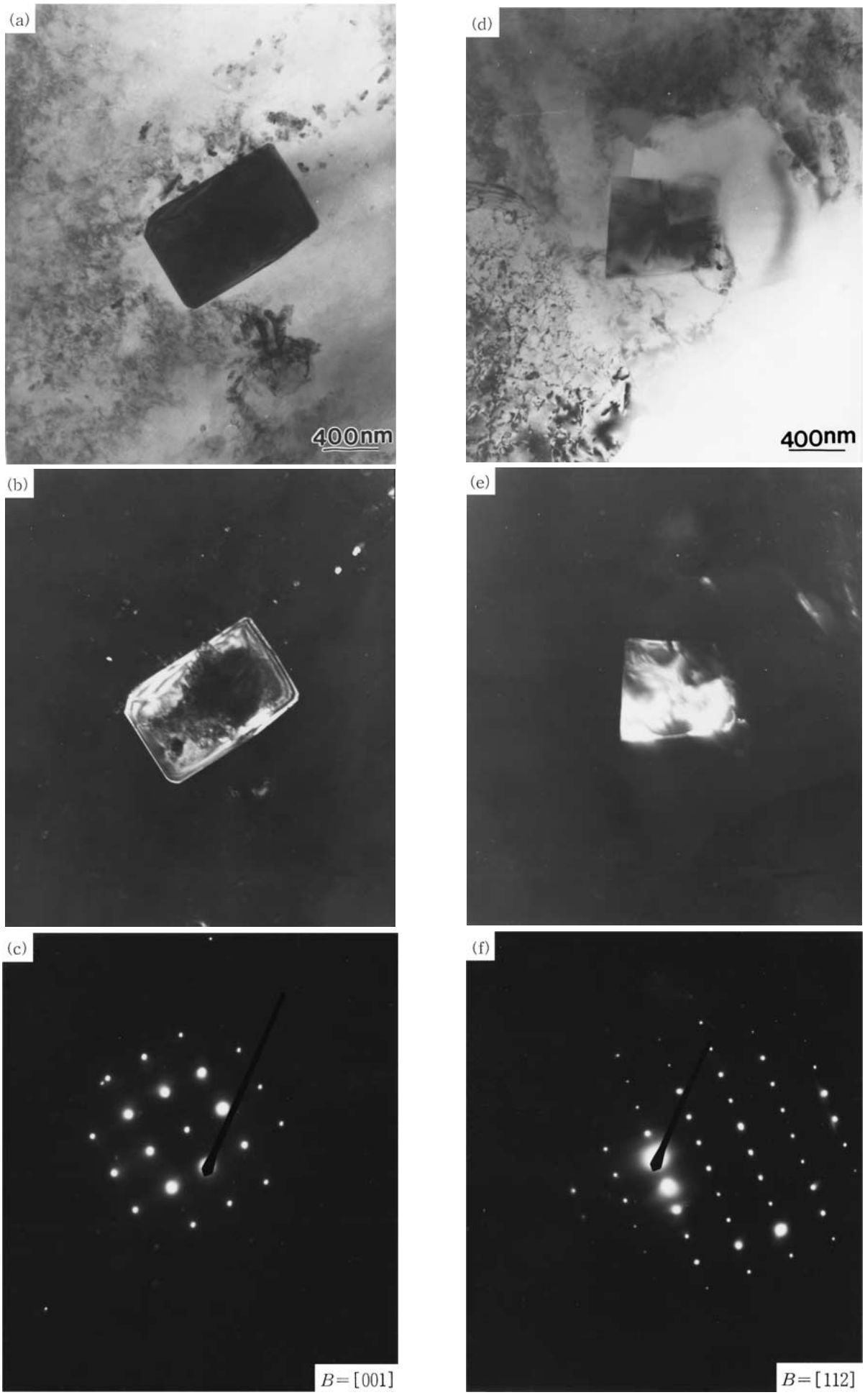

Figure 7 TEM micrographs showing reaction product, $MgAl_2O_4$: (a) BF, (b) DF, and (c) SADP in control alloy, and (d) BF, (e) DF, and (f) SADP in the composite, respectively.

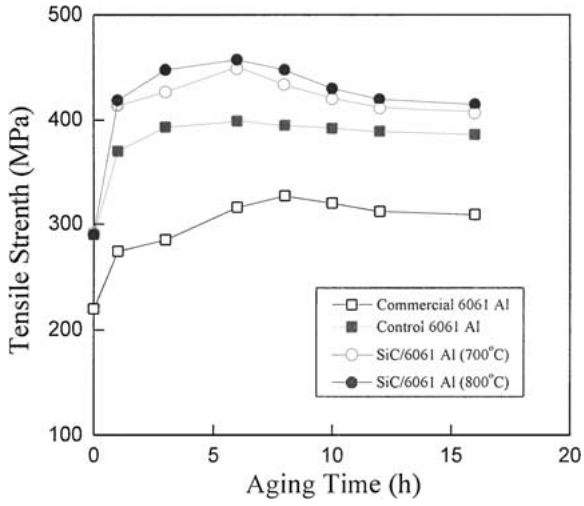

Figure 8 Tensile strength variation with aging time after a solution heat treatment of 2 h at 529 °C.

the composite fabricated at 700 °C. While the strength values in both composites exhibited similar to each other, particularly, strain to failure of the composite fabricated at 800 °C showed the lowest value (1.3%) in the T6 condition. This means that the reaction products (Al_4C_3) have significant effect on the ductility rather than strength. The fracture surfaces of the composites are shown in Fig. 10. It is observed that particle cracking much more pronounced in the composite fabricated at 800 °C.

In addition, since aging kinetics was accelerated by the formation of AlN as well as by the addition of SiC, the time to peak strength decreased in both control alloy and composite. Fig. 11 is TEM micrographs showing Mg_2Si precipitates in the commercial, control alloy, and composite in the T6 condition, respectively. The Mg_2Si precipitates formed in the composite was finer and denser when compared to the alloy.

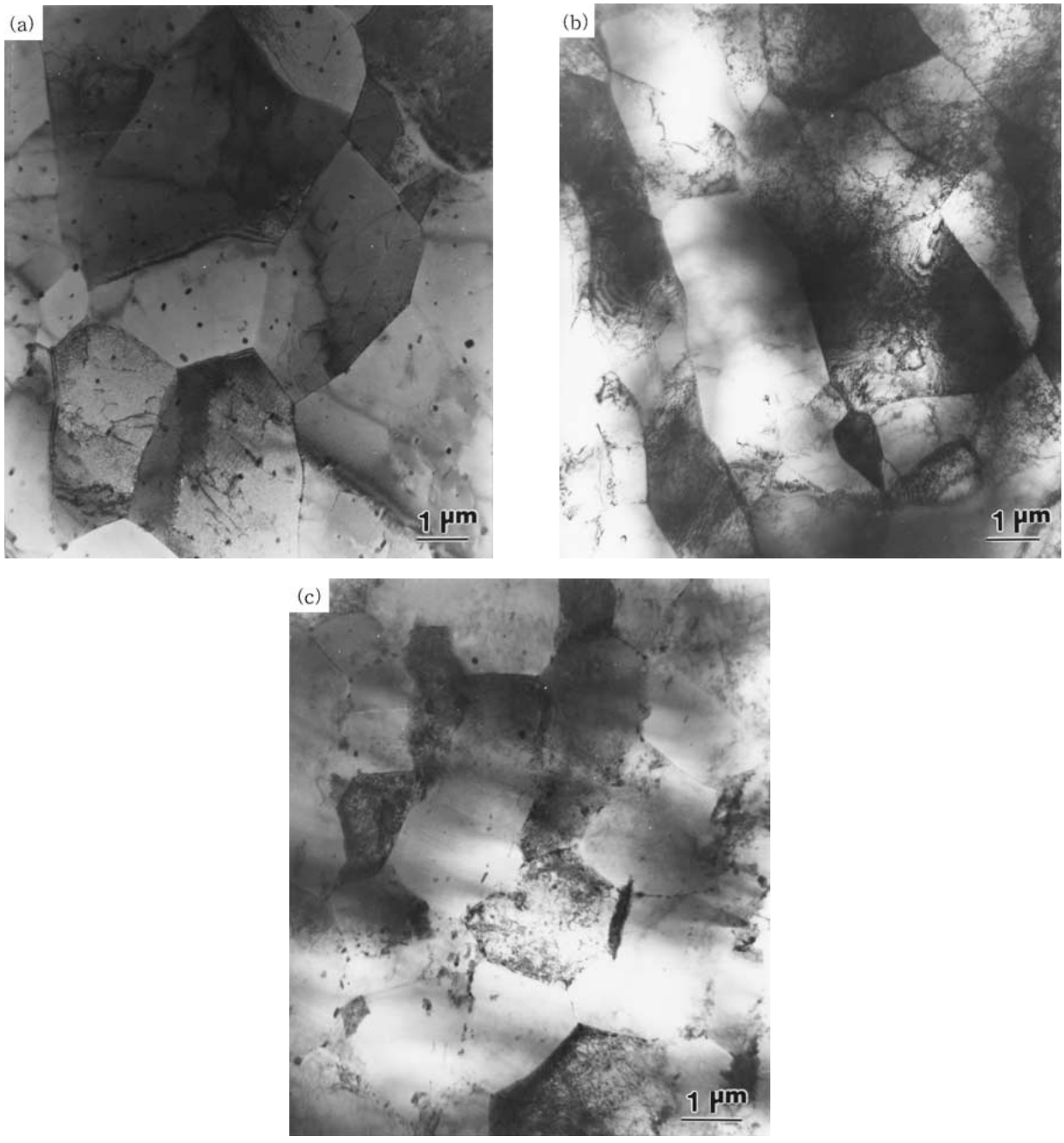

Figure 9 TEM micrographs showing the subgrain structure: (a) commercial, (b) control alloy, and (c) composites, respectively.

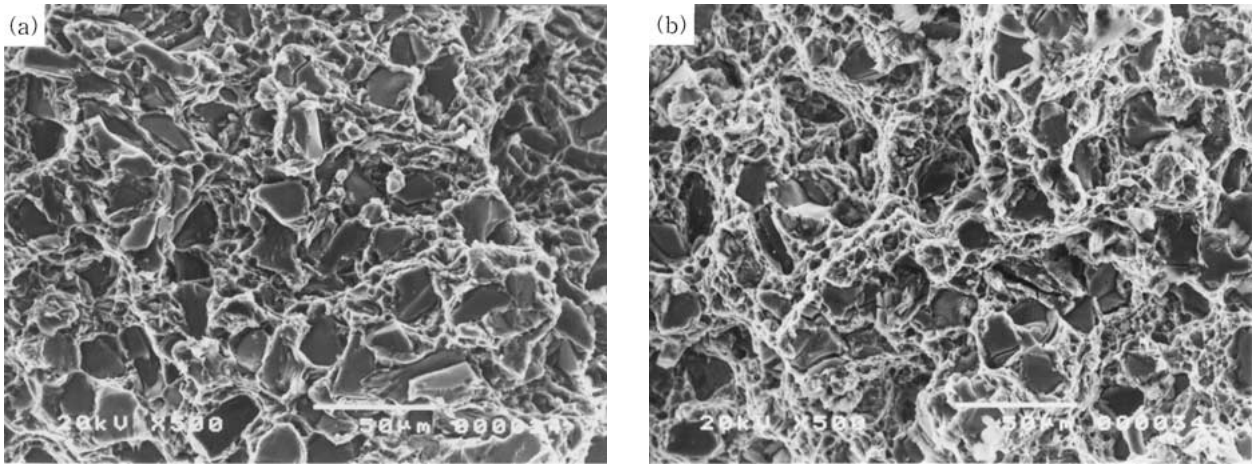

Figure 10 SEM fractographs showing fracture surfaces of the composites fabricated at 700 °C (a) and 800 °C (b), respectively.

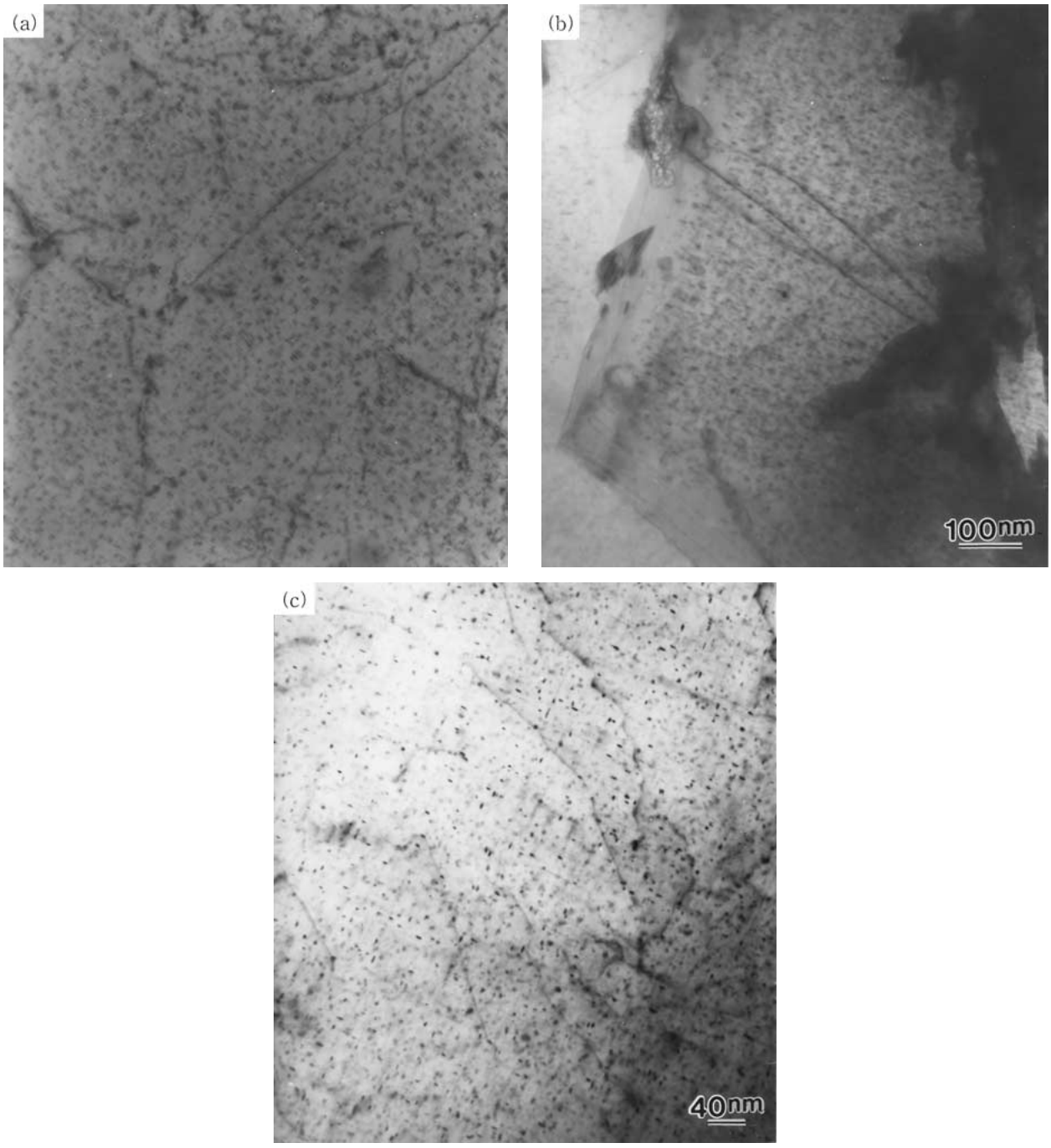

Figure 11 TEM micrographs showing the Mg_2Si precipitates in the T6 condition: (a) commercial, (b) control alloy, and (c) composite, respectively.

4. Conclusions

The tensile properties and microstructures of AA6061/SiC_p composites fabricated by the pressureless infiltration method under a nitrogen atmosphere were examined. Since the spontaneous infiltration of molten AA6061 into the powder bed containing SiC_p occurred at 800 °C for 1 hour under a nitrogen atmosphere, it was possible to fabricate composites reinforced with SiC_p. Reaction product (Al_4C_3) was formed at the interface between SiC_p and Al alloy matrix. In addition, the amount and size of the Al_4C_3 is increased significantly by increasing the infiltration temperature.

The reaction product (AlN) was formed as a result of the *in situ* reaction in both the control alloy and the composite. A significant strengthening even in the control alloy occurred due to the formation of *in situ* AlN particle even without an addition of SiC_p. While a further strengthening of the composite was produced by the reinforced SiC_p, strain to failure of the composite fabricated at 800 °C showed the lowest value (1.3%) in the T6 condition due to the formation of the severe reaction product (Al_4C_3). The grain size of the control alloy significantly decreased to about 20 μm compared to 50 μm for the commercial alloy. In addition, the grain size in the composite reinforced with SiC_p further decreased to about 8.0 μm. These grain refinement contributed to strengthening of the control alloy and composite.

Acknowledgment

This work was supported by the Korea Science and Engineering Foundation (KOSEF: 97-0300-07-01-3).

References

1. A. MORTENSEN and I. JIN, *Int. Mater. Rev*. **37** (1992) 101.
2. A. IBRAHIM, F. A. MOHAMED and E. S. LAVERNIA, *J. Mater. Sci*. **26** (1991) 1137.
3. M. J. KOCZAK and M. K. PREMKUMAR, *J. Metall.* **45** (1993) 44.
4. R. ASTHANA, *J. Mater. Sci*. **33** (1998) 1679.
5. M. K. AGHAJANIAN, J. T. BURKE, D. R. WHITE and A. S. NAGELBERG, *SAMPE Q* **20**(4) (1989) 43.
6. M. K. AGHAJANIAN, M. A. ROCAZELLA, J. T. BURKE and S. D. KECK, *J. Mater. Sci*. **6** (1991) 447.
7. A. W. URQUHART, *Advanced Mater. Process*, July (1991) 25.
8. *Idem*., *Mater. Sci. Eng*. **144** (1991) 75.
9. R. E. EVERETT and R. J. ARSENAULT, in "Metal Matrix Composites: Processing and Interfaces" (Academic Press, 1991) p. 121.
10. M. K. AGHAJANIAN, A. S. NAGELBERG and C. R. KENNEDY, U.S Patent no. 5020584.
11. K. B. LEE, Y. S. KIM and H. KWON, *Metall. Mater. Trans. A* **29** (1998) 3087.
12. K. B. LEE and H. KWON, *ibid.* **30** (1999) 2999.
13. K. B. LEE, H. S. SIM, S. W. HEO, S. Y. CHO and H. KWON, *Korea Inst. Metall & Mater*. **6** (2000) 25.
14. K. B. LEE, J. P. AHN and H. KWON, *Metall. Mater. Trans. A* **32** (2001) 1007.
15. K. B. LEE, H. S. SIM, S. Y. CHO and H. KWON, *Mater. Sci. Engr*. **302** (2001) 227.
16. J. C. LEE, J. Y. BYUN, S. B. PARK and H. I. LEE, *Acta Mater*. **46** (1998) 1771.
17. V. MASSARDIER and P. MERLE, *Mater. Sci. Engr*. **249** (1998) 109.
18. W. M. ZHONG, G. L'ESPÉRANCE and M. SUÉRY, *Metall. Mater. Trans. A* **26** (1995) 2637.
19. J. C. VIALA, F. BOSSELET, V. LAURENT and Y. LEPETITCORPS, *J. Mater. Sci*. **28** (1993) 5301.
20. R. Y. LIN and K. KANNIKESWARAN, in Proc. Int. Conf. on Interface in Metal-Ceramic Composites, Anaheim, CA, February 1990, edited by R. Y. Lin, R. J. Arsenault, G. P. Martins and S. G. Fishman (TMS, 1990) p. 153.
21. G. SELVADURAY, R. HICKMAN, D. QUINN, D. RICHARD and D. ROWLAND, in Proc. Int. Conf. on Interface in Metal-Ceramic Composites, Anaheim, CA, February 1990, edited by R.Y. Lin, R.J. Arsenault, G. P. Martins and S. G. Fishman (TMS, 1990) p. 271.
22. "CRC Materials Science and Engineering Handbook," edited by J. F. Shackelford, W. Alexander and J. S. Park (1994) p. 43.
23. W. M. ZHONG, G. L'ESPÉRANCE and M. SUÉRY, *Mater. Sci. Engr*. **93** (1996) 93.
24. F. J. HUMPHREYS, W. S. MILLER and M. R. DJAZEB, *Mater. Sci. Technol*. **6** (1990) 1157.
25. M. FERRY, P. MONROE, A. CROSKY and T. CHANDRA, *ibid*. **8** (1992) 43.

Received 10 January
and accepted 12 February 2001